Structural Analysis of Historic Construction – D'Ayala & Fodde (eds)
© 2008 Taylor & Francis Group, London, ISBN 978-0-415-46872-5

Capacity of a traditional timber mortise and tenon joint

Artur O. Feio
Madeicávado – Madeiras, S. A. University Lusíada, Famalicão, Portugal

Paulo B. Lourenço
University of Minho, Guimarães, Portugal

José S. Machado
LNEC, Lisboa, Portugal

ABSTRACT: The safety and quality of traditional timber structures mostly depends on the conditions of their connections. A testing campaign has investigated the behaviour of mortise and tenon timber joint. The present paper addresses the quantification of the strength capacity of wood-wood mortise and tenon joint by physical testing of full-scale specimens. In addition, the performance of different non-destructive techniques (NDT) for assessing global strength is also evaluated. For this three non-destructive methods (ultrasonic testing, Resistograph and Pilodyn) are considered and the possibility of their application is discussed based on the application of simple linear regression models. New (NCW) and old (OCW) chestnut wood, obtained from structural elements belonging to old buildings, is used. Finally, a nonlinear model has been formulated and the predicted behaviour compared with the behaviour observed in the full-scale experiments, in terms of failure mode and the ultimate load. The study has shown very good agreement with the experimental values.

1 INTRODUCTION

In the past, timber structural design was dominated by the carpenter know-how which in turn was based upon his previous works or upon the works of others both supported on timber trusses solutions that performed reasonable well (did not fall). Although carpenters awareness that some members were subjected to tension and others to compression stresses is evident from the observation of old timber structures. Joints assure important functions as holding on the truss and sustaining the stresses imposed on it. In traditional timber constructions load distribution through joints was made with empirical knowledge, transmitted and improved through generations. The early design rules or standards were built upon this empirical evidence.

The mortise and tenon joint was selected because it is one of the most commonly used and a typical example of an interlocking joint. Mortise and tenon joints were the basic components of joint craftery in Portugal and connect two or more linear components, forming a "L" or "T" type configuration, see Figure 1. The key problem found in these joints is the possible premature failure caused by large displacements. Unlike most timber joints, the load-displacement behaviour of these joints is generally very ductile.

The bearing capacity of mortise and tenon joints is a function of the angle of the connection, and length of the toe and mortise depth. According to the European building codes, joints are of crucial importance for the seismic design of timber structures. However, there are no recommendations on the design codes about general dimensions, such as length of the toe and the mortise depth in order to avoid structural failure of the connections, and the joints in existing structures are based on empirical rules.

Therefore, the present study addresses such type of joints. In particular, the objective is: (a) to investigate the static behaviour of real scale replicates, considering both new (NCW) and old (OCW) timber connections (wood-wood connections) of chestnut wood (*Castanea sativa* Mill.); (b) to characterize the ultimate strength and, the global deformation of the joint, as well as the respective failure patterns; and (c) to verify the impact of time and loading history in the strength and stiffness. For these purposes, the paper presents several correlations between mechanical properties, density and non destructive methods.

The adopted non-destructive methods for the joints are the Pilodyn, Resistograph and ultrasonic tests. These *in situ* methods allow to assess the safety of old structures and preserve the original fabric as much as possible, representing a first step towards diagnosis, structural analysis and the definition of possible remedial measures (Ross *et al*. 1997). The inspection results, combined with historical information and

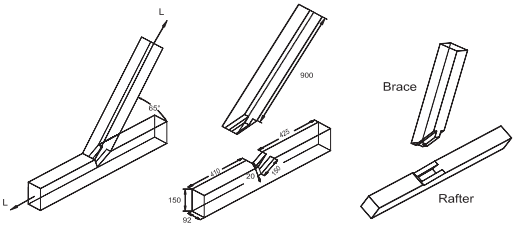

Figure 1. Details of typical tenon and mortise joints.

a visual survey, can also be the support of maintenance decisions. Non-destructive evaluation is already widely applied to the control of structural integrity, due its characteristics of reliability, simplicity and low cost.

For the purpose of numerical analysis wood is often considered as a homogenous and isotropic material. This is certainly not the case as: (a) wood exhibits anisotropic elastic and inelastic behaviour; (b) natural growth characteristics such as knots, slope grain and other defects are always present. Defects can be included in numerical simulations but this requires a thorough investigation of the specimens and fine tuning, being of moderate interest for practical purposes. On the contrary, the usage of orthotropic failure criteria is essential for accurate numerical simulations.

Failure criteria that describe orthotropic inelastic behaviour offer the opportunity to perform adequate analyses of wood elements and structures, beyond the elastic limit. This can be especially valuable in the detailed analysis of timber joints and other details with complex stress distribution.

Here, the finite element method (FEM) is adopted to simulate the structural behaviour and obtain a better understanding of the failure process. Calculations are performed using a plane stress continuum model, which can capture different strengths and softening/hardening characteristics in orthogonal directions. The failure criterion is based on multi-surface plasticity, comprising an anisotropic Rankine yield criterion for tension, combined with an anisotropic Hill criterion for compression.

The failure criterion from Lourenço (1996) is used in the analysis. The influence of compression perpendicular to the grain and elastic stiffness on the response is addressed in detail.

2 DESCRIPTION OF THE TEST SPECIMENS

Chestnut is usually present in historical Portuguese buildings and all the wood used in the specimens came from the North of Portugal. The 8 specimens were divided in two groups: New Chestnut Wood (NCW), obtained from recently sawn timber, and Old Chestnut Wood (OCW), obtained from structural elements belonging to old buildings (date and precise origin unknown). The old logs were obtained from a specialist contractor claiming that the wood has been in service for over 100 years. The OCW specimens were made using original beams obtained from rehabilitation works carried out in the Northern of Portugal, using specimens with the least possible damage. The NCW specimens were prepared using new wood with minor defects.

Table 1. Average values of density (one specimen for each timber element).

	Density (kg/m^3)				
	Brace	Rafter	Average	Std. Dev.	Group
J_1	584.2	602.1	593.6	25.4	**NCW**
J_2	584.9	544.2			
J_3	604.0	605.5			
J_4	590.2	633.3			
J_5	575.1	605.6	568.8	31.4	**OCW**
J_6	598.9	574.7			
J_7	507.1	545.7			
J_8	561.7	581.8			

Attention was paid to the conditioning of the timber before and after the manufacture of the joints. The conditioning was conducted in such a way that the test conditions correspond in a realistic manner to adequate *in situ* conditions as regards the influence of moisture content and the occurrence of gaps induced by shrinkage.

Each specimen consists of two timber elements, with a cross section of $92 \times 150\,\text{mm}^2$, connected with a mortise and tenon joint without any pins. The angle between the elements is 65°.

3 CHARACTERIZATION OF PHYSICAL AND MECHANICAL PROPERTIES

3.1 *Density*

Given the conditioning of the specimens, the average density ρ_m is determined for a moisture content of 12%. Table 1 presents the results for the average density organized according to two group types (wood element and age). The density tests were carried out in samples removed from the specimens ends. Even if the sample size is very low, the NCW group presents slightly higher values of average density (≈4%) than OCW group, with an average of 593.6 kg/m^3 for NCW and 568.8 kg/m^3 for OCW.

3.2 *Experimental tests*

A test set-up was built to test the specimens under compression. One hydraulic jack was used to apply a compression force aligned with the rafter, with a programmed loading cycle. The system includes a support plate with stiffeners, able to rotate and ensure

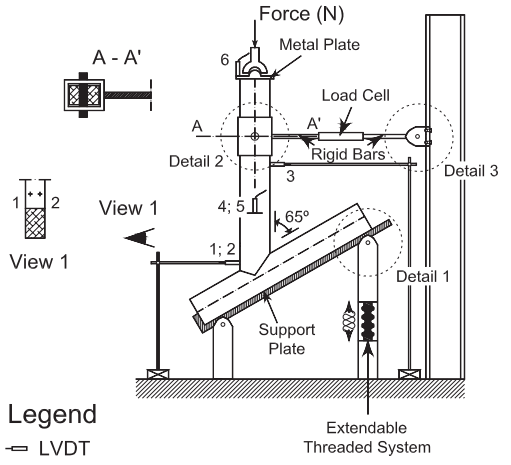

Figure 2. Aspects of the destructive test set-up.

verticality of the brace. The support plate includes a toe so that the rafter does not suffer a displacement along its axis. The brace is hold in the original alignment with a horizontal bar, connected to a load cell. Additionally a feed, acquisition and amplification data system was used, to obtain and to register all the data, see Figure 2.

Displacements were measured using linear variable differential transducers (LVDT), continuously recorded until failure occurred. The measurements of the vertical and horizontal displacements in the specimens were done by two pairs of LVDT's placed on opposite faces of the specimens to eliminate the effect of bending (if any).

The loading procedure consisted of the application of 2 monotonic load stages: firstly, the load was applied up to 50% of the estimated maximum load (determined on the basis of the preliminary tests) and was maintained for 30 s. The load was then reduced to 10% of the estimated maximum load and maintained for 30 s. This procedure was repeated once again and, thereafter, the load was increased until ultimate load or until a maximum slip of 15 mm between the two timber elements was reached. This is based on the EN 26891 (1991) requirements.

A constant rate of loading corresponding to about 20% of the estimate maximum load per minute was used, in such a manner that the ultimate load or slip of 15 mm was reached in about five minutes of additional testing time in the final loading procedure. The total testing time is about 9 to 12 minutes. The ultimate load of the joint ($F_{ult,joint}$) is defined as the conventional value corresponding to a strain equal to a 2% offset in the usual terminology.

3.2.1 *Results*

The results of the experimental tests are presented in Table 2. It can be seen that the results presents a huge

Table 2. Average values of density (one specimen for each timber element).

	Ultimate Force (kN)	Average	Std. Dev.	Group
J_1	121.6	145.4	18.9	**NCW**
J_2	161.5			
J_3	159.7			
J_4	138.9			
J_5	126.4	133.8 (145.5*)	27.2 (16.7*)	**OCW**
J_6	157.1			
J_7	98.5			
J_8	153.0			

(*) average discarding specimen J_7.

Figure 3. Typical experimental failure patterns: joint collapsed in compression, with uniform distribution of damage.

scatter, ranging from an ultimate force of 98.5 kN up to a force of 161.5 kN. Even if the number of specimens is rather low, the average force in terms of groups NCW and OCW exhibits a difference lower than 10%. Specimen J_7 can possibly be discarded because the value found is too low and is controlled by a local defect: the large longitudinal crack in the rafter. In this case, the average ultimate force values of the groups NCW and OCW are almost the same.

The main characteristic of the adopted joint is that the direction of the grain of the two assembled pieces it is not coincident, forming an acute angle. The rafter is loaded in the direction parallel to the grain, whereas the brace is loaded at an oblique angle inducing large stresses perpendicular to the grain. Due to the anisotropic behaviour of wood, wood stressed parallel to the grain assumes the highest values of strength. Therefore, the rafter, stressed in compression parallel to the grain, easily penetrates the brace. The compressive damage in the brace occurred either localized at the toe or distributed along the full contact length. Often, out-of-plane bulging of the rafter under the contact length was observed. In some cases, compressive damage was accompanied with shear failure in the rafter in front of the toe. Figure 3 illustrates the typical damage observed at ultimate load and gives the experimental results in terms of ultimate force.

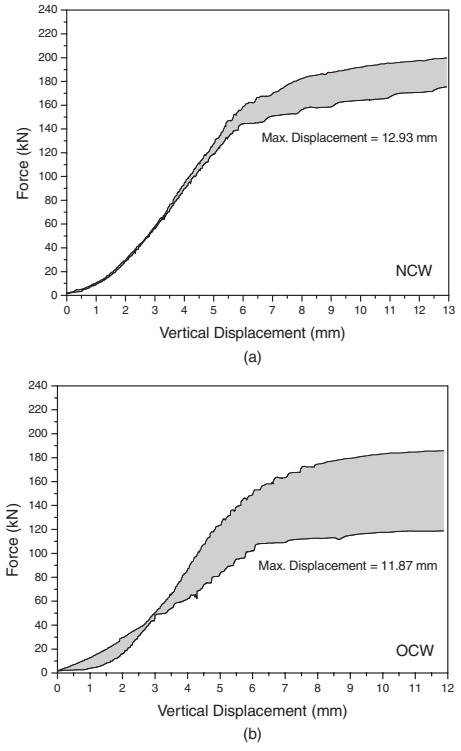

Figure 4. Envelope of load-displacement diagrams for: (a) the NCW group, and (b) the OCW group.

The specimens were executed avoiding the presence of large defects but some small defects were present. During the tests it was observed that the longitudinal and radial cracks of moderate width in the rafter did not have a considerable influence in the ultimate strength and in the global behaviour of the joints. The longitudinal cracks show the tendency to close their thickness and the radial cracks show the tendency to open. This effect is more salient when the cracks are close to the joint. On the other hand, the cracks present in the brace, namely the longitudinal ones, show a tendency to propagate and to open during the tests. Nevertheless, it seems difficult to quantify the influence of these cracks in the ultimate strength of the joint.

3.2.2 *Load-displacement diagrams*

The difference in the results between old and new wood is very low, which seems in agreement with the values of density found for the sample, where the NCW group present slightly higher values of density (≈5%) in comparison with the OCW group.

The results of all tests in terms of load-displacement diagrams, given by the vertical force vs. vertical displacement, are given in Figure 4.

Figure 4a and Figure 4b show typical individual load-displacements diagrams and envelopes of load-displacement diagrams. It is evident as addressed before, that the scatter of the OCW group is much larger than the scatter of NCW group, due to J_7 specimen. From the load-displacement diagrams obtained the following relevant remarks can be drawn. In a first phase, the diagrams always start with an upward curvature, exhibiting a nonlinear, non-recoverable, "bedding" response, which is due to the adjustment of the tenon and the mortise. In a second phase, within working stress levels, the response exhibits an approximately linear branch up to the conventional maximum load, which occurred at an average displacement of 8 mm for the NCW group and 7 mm for the OCW group. The value of the displacement associated with the maximum load is lower for the NCW group joints in comparison with the OCW group joints, possibly indicating a slightly larger deterioration of the timber of the OCW specimens. It is noted that unloading-reloading cycles within working stress levels provide a constant stiffness, which is higher than the loading stiffness. The justification of this behaviour is probably attributed to the nonlinear behaviour of the interface between rafter and brace, which exhibits a closure phenomenon. Finally, after the conventional maximum load the displacement increases rapidly with a much lower stiffness, due essentially to the compressive failure of the wood in the rafter around the joint.

For the purpose of a more refined numerical analysis, the true load-displacement diagrams were corrected with an offset that eliminates the upward curve related to the nonlinear behaviour of the joint previous to full contact (joint closure).

Due to the nature of load-displacement diagrams for these joints, choosing the linear portion of the curve includes some subjectivity. To reduce the subjectivity the elastic stiffness was calculated between 1/3 and 2/3 of the ultimate load. The line plotted between these two points to visually analyze the quality of the fit to the linear portion of the plot, indicated that the proposed procedure is adequate.

4 DESCRIPTION OF NON-DESTRUCTIVE TEST PROCEDURES

In order to investigate possible correlations and the validity of using NDE as a tool to assess the joint strength, different non-destructive techniques (NDT's) have been carried out. The adopted NDT's are the Pilodyn, the Resistograph and the ultrasonic tests, which were carried out in both timber elements. Average values were considered in all measurements and two readings per specimen, per side, were generally made but a third one was added if the two first readings differed significantly. Here, it is noted that Pilodyn and Resistograph have been carried out in samples removed from the elements ends, in order not to affect

Table 3. Average results of the Resistograph and Pilodyn Tests (values in bits/mm and mm, respectively).

	Resistograph		Pilodyn		
	Brace	Brace	Rafter	Rafter	Group
J_1	449.5	449.5	8.0	8.0	NCW
J_2	367.7	367.7	7.8	8.8	
J_3	365.0	365.0	8.0	7.3	
J_4	463.6	463.6	8.0	7.3	
J_5	391.7	391.7	8.0	8.2	OCW
J_6	332.0	332.0	8.0	7.3	
J_7	396.6	396.6	9.0	8.8	
J_8	323.1	323.1	8.7	8.2	

(even if marginally) the local strength of the joint, and the ultrasonic tests have been carried out at the exact joint location.

4.1 *Pilodyn and resistograph tests*

The results shown represent therefore the average of the readings permitting to reduce the scatter related to local measurements.

The resistographic drills were made by using the Resistograph 3450-S. For all the specimens, a resistographic measure (RM) was calculated from the diagram obtained with the Resistograph (see Feio *et al.*, 2005), as the ratio between the integral of the area of the diagram and the length l of the drilled perforation. The average results are presented in Table 3.

The Pilodyn 6J can measure the penetration of a metallic needle with 2.5 mm of diameter, which is inversely proportional to the density of the wood, evaluating the surface hardness or resistance to superficial penetration. The average results are presented in Table 3.

4.2 *Ultrasonic tests*

Given the dimensions of the wood elements and the diameter of the transducers used (ϕ = 25 mm), a reference testing mesh was defined on the central mid-third of each element.

The tests in the brace and rafter aimed at characterizing the mechanical properties of the elements in zones nearby the joint. The test across the joint tried to evaluate in a qualitative way the effectiveness of the assembly between the two elements. A through-transmission technique was adopted measuring the wave propagation velocity parallel to the grain in each element and joint.

A Pundit/Plus device (ultrasound generator) and a pair of cylinder-shaped transducers (150 kHz) were used. In all tests, coupling between the transducers and specimens was assured by a conventional hair gel, and a constant coupling pressure was applied on top of the transducers by means of a rubber spring. The transducers were fixed into a special purpose assembly jig to ensure their alignment.

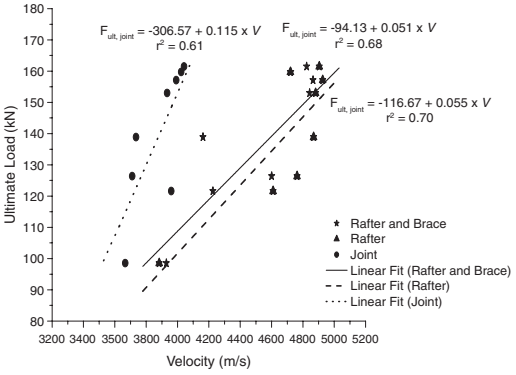

Figure 5. Ultrasonic pulse velocity method for all tests: relation between the ultimate load and the ultrasonic pulse velocity.

4.3 *Results*

The results indicated that these non-destructive techniques (Pilodyn and Resistograph method) are not good indicators for predicting the joint strength. Again, a definitive conclusion cannot be made because the measurements had been made in specimens ends and not at the joint location. However, taking into account also the previous Chapters, these non-destructive techniques seem more adequate to make a preliminary estimation of density, rather than mechanical grading of wood.

Figure 5 illustrates the relation between the ultimate load and the ultrasonic pulse velocity. The results show that ultrasonic pulse velocity could be a good indicator for the prediction of the ultimate load. Here, it is noted that the results using local measurements only in the rafter, or rafter and brace together provide better correlations that measurements across the joint. In the latter, also the stiffness of the joint is taken into account, meaning that the ultrasonic pulse velocity is much lower. The joint stiffness is a relevant parameter for the estimation of deformations and, sometimes, resistance of timber structures. A clear linear correlation was found, indicating that it is possible to estimate joint stiffness from ultrasonic testing.

5 NUMERICAL ANALYSIS

In structural mechanics, a problem is usually considered to be nonlinear if the stiffness matrix or the load vector depends on displacements. Nonlinearities in a structure can be typically classified as material or as geometric nonlinearities.

Table 4. Adopted elastic and inelastic material properties.

E_x	E_y	G_{xy}	ν_{xy}
800 N/mm^2	8500 N/mm^2	1500 N/mm^2	0.3
$f_{c,x}$	$f_{c,y}$	β	γ
7 N/mm^2	45 N/mm^2	−1.0	3.0

Nonlinear analysis is used to trace the equilibrium path up to and beyond the first critical point, at which the structure becomes unstable. There is one algorithm commonly used in the incremental iterative solution of nonlinear problems: the Newton-Raphson method. The full Newton-Raphson method, with stiffness matrix update in each iteration is used in the analyses carried out in this work.

Two different finite elements were considered in the plane stress analyses carried out in this work: continuum elements (8-noded) to represent wood and line interface elements (6-noded) to represent the interface between rafter and brace. The integration schemes used are 2×2 Gauss integration points for the continuum elements and 3 Lobatto integration points for the interface elements.

5.1 *The adopted anisotropic failure criteria*

A plane stress continuum model, which can capture different strengths and softening characteristics in orthogonal directions, was formulated by Lourenço (1996). The proposed failure criterion consists of an extension of conventional formulations for isotropic quasi-brittle materials to describe orthotropic behaviour. It is based on multi-surface plasticity, and wood is an example of a material for which this criterion applies, having different strengths in the directions parallel and perpendicular to the grain.

Formulations of isotropic quasi-brittle materials behaviour consider, generally, different inelastic criteria for tension and compression. In this formulation, and in order to model orthotropic material behaviour, a Hill yield criterion for compression and a Rankine yield criterion for tension were adopted.

5.2 *Adopted material parameters*

A characteristic of the adopted model is that the tension strength, in a given direction, must be equal or lower to the compression strength in the same direction. This does not hold for wood. Here, the tensile part of the yield criterion was ignored due to the irrelevant contribution of the tensile strength in the global behaviour of the joint. This means that the yield surface reduces to the standard Hill criterion. The adopted elastic and inelastic materials properties used in the analyses are detailed in Table 4.

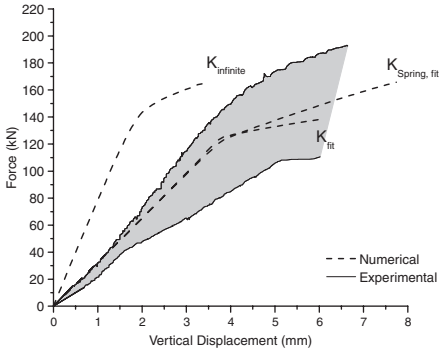

Figure 6. Comparison between numerical and experimental load-displacement diagrams.

The shape of the adopted yield criterion in the compression-compression regime, features an extreme degree of anisotropy with a ratio $f_{c,x}/f_{c,y} = 0.156$.

6 NUMERICAL VS. EXPERIMENTAL RESULTS

A structured mesh is used for the rafter and the brace, whereas an irregular transition mesh is used in the vicinity of the connection between rafter and brace. Interface elements are also used between the rafter and the brace. The thickness ranges from 62 mm to 93 mm. This aims at representing the thickness of the mortise.

A preliminary analysis with an infinite stiffness of the interface, assuming a fully rigid connection, indicated that such an assumption provided far too stiff results. Therefore, the stiffness of the interface elements was obtained by inverse fitting. A first conclusion is that the stiffness of the interface elements has considerable influence in the yield strength of timber joints. In Figure 6, three distinct situations are presented: a numerical simulation with infinite stiffness of the interface elements ($k_{infinite} = k_n = k_s = 10^9$ N/mm^3); a numerical simulation with an adjusted stiffness of the interface elements obtained by inverse fitting of the experimental results (k_{fit}): $k_n = 6000$ N/mm^3 and $k_s = 2308$ N/mm^3; and a numerical simulation with a spring ($k_{spring} = 10^6$ N/m) located in the brace to simulate the reaction cell used in the experimental sets. The stiffness of the spring was again obtained by inverse fitting of the experimental results, keeping the adjusted stiffness of the interface elements.

The numerical results, in terms of force-displacement diagrams, with the adjusted stiffness for the interface elements, provide very good agreement with the experimental results both in the linear and nonlinear parts. The influence of the experimental horizontal restraint, simulated by a linear spring, is only

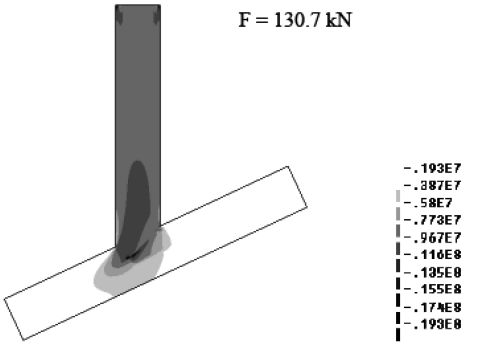

Figure 7. Minimum principal stresses (values in N/mm^2).

marginal. The usage of infinite stiffness for the interface (rigid joint) results in an increase of the slope of the first part of the response, from 30 kN/mm to 80 kN/mm (+266.7%). The ultimate strength of the joint, given by an offset of the linear stretch by 2% in terms of strain values, also changes from 130 kN to 152 kN (+17%), once the joint becomes fully rigid.

Figure 7 shows the contour of minimum principal stresses at the end of the analysis. It is possible to observe a concentration of stresses in a narrower band with peak stresses at the joint (zone where the interface elements were placed).

With this concentration of stresses one may say that failure is clearly governed by wood crushing where, for a late stage of the analysis, the compressive strength of the wood in the joint is completely exhausted. This situation is also confirmed in the experiments.

7 EFFECTS OF THE MATERIAL PARAMETERS

A strong benefit of using numerical simulations is that parametric studies can be easily carried out and the sensitivity of the response to the material data can be assessed. There are a total of six key parameters in the present model and the effect of each parameter on the global response will be analyzed separately. It is noted that moderate variations (±25%) are considered for the strengths and large variations (division/multiplication by two) are considered for the stiffness values. These assumptions are rooted in the fact that strength is usually better known than stiffness.

7.1 *Normal stiffness of the interface*

Figure 8a shows a comparison between the results of the variation of the k_n parameter: with a reduction of 50% in k_n, the ultimate strength of the joint, given by an offset of the linear stretch by 2%, decreases from 127.2 kN to 120 kN (−6%); multiplying k_n by a factor of two the ultimate strength of the joint, given by

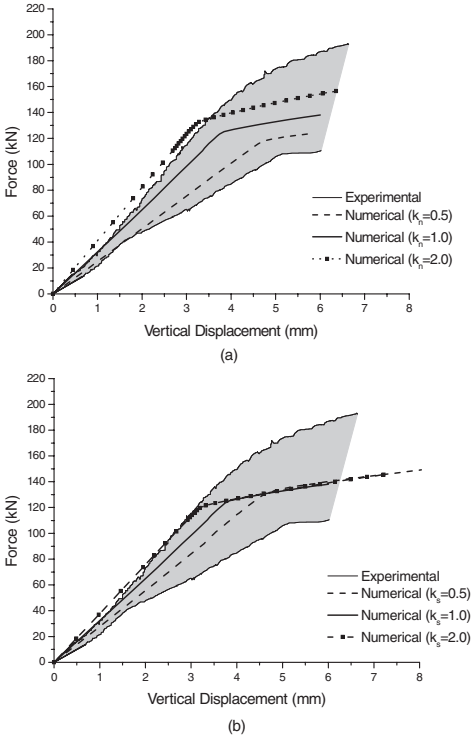

Figure 8. Effect of the variation of parameter: (a) k_n, and (b) k_s on the model response.

an offset of the linear stretch by 2%, increases from 127.2 kN to 135.0 kN (+7%).

The reduction/increase of the normal stiffness of the interface also affects the global stiffness of the joint: the global stiffness of the joint decreases as the normal stiffness of the interface decreases, being more sensitive to this variation when compared with the ultimate strength. The reduction of 50% of the k_n parameter, results in a decrease of the slope of the first part of the response, from 32 kN/mm to 26 kN/mm (−23%).

On the other hand, the multiplication by a factor of 2 of this parameter results in an increase of the slope of the first part of the response, from 32 kN/mm to 41 kN/mm (+28%). Because this parameter sets the relation between the normal traction and the normal relative displacement, the obtained results were expected *a priori*.

7.2 *Tangential stiffness of the interface*

Figure 8b shows a comparison between the results of the variation of the k_s parameter. The ultimate strength is insensitive to a k_s variation, whereas the reduction/increase of the k_s parameter affects the global stiffness of the joint: the global stiffness of the joint

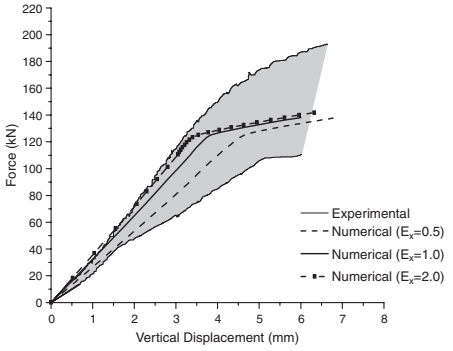

Figure 9. Effect of the variation of the elastic modulus of elasticity (E_x) on the model response.

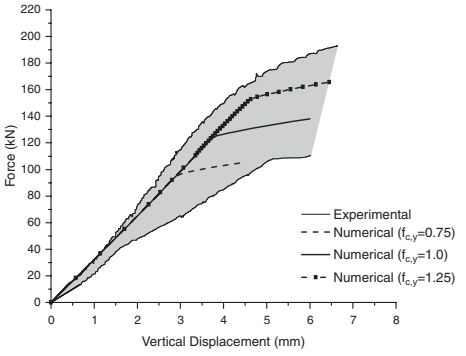

Figure 10. Effect of the variation of the compressive strength ($f_{c,y}$) on the model response.

decreases as the k_s parameter decreases. The reduction of 50% of the k_s parameter, results in a decrease of the slope of the first part of the response, from 32 kN/mm to 28 kN/mm (−14%).

On the other hand, the multiplication by a factor of 2 of this parameter results in an increase of the slope of the first part of the response, from 32 kN/mm to 37 kN/mm (+16%).

7.3 *Elastic modulus*

The effect of the variation of the elastic modulus of elasticity parallel and perpendicular to the grain was considered individually. Figure 9 indicates that the ultimate strength is almost insensitive to the variation of the elastic modulus of elasticity for wood (± 4%).

The inclusion of the effects of the elastic modulus of elasticity does change significantly the elastic stiffness of the joint. Therefore, decreasing the parameter E decreases the global stiffness of the joint. The reduction of 50% of the E_x parameter, results in a decrease of the slope of the first part of the response, from 32 kN/mm to 28 kN/mm (−14%). On the other hand, the multiplication by a factor of 2 of this parameter results in an increase of the slope of the first part of the response, from 32 kN/mm to 36 kN/mm (+13%).

7.4 *Compressive strength*

The ultimate strength and the global stiffness of the joint are insensitive to the variation of the compressive strength of wood in the parallel direction.

Figure 10 indicates higher sensitivity of the ultimate strength of the joint to the variation of the compressive strength of wood in direction perpendicular to the grain, as expected: with a reduction of 50%, the ultimate strength of the joint, given by an offset of the linear stretch by 2‰, decreases from 130 kN to 100 kN (−30%); multiplying by a factor of 2 the ultimate strength of the joint, given by an offset of the linear stretch by 2‰, increases from 130 kN to 160 kN (+23%). However, the global stiffness of the joint is insensitive to the variation of the compressive strength perpendicular to the grain.

8 CONCLUSIONS

Despite the wide use of mortise and tenon joints in existing timber structures scarce information is available for design and *in situ* assessment. The objective of the present study was to quantify its strength capacity by physical testing of full-scale specimens. Also, the performance of different NDT for assessing global joint strength is evaluated. Finally, the adequacy of an anisotropic failure criterion to represent the behaviour of a traditional mortise and tenon joint was assessed from the comparison between experimental and numerical results.

The difference in the results for the ultimate load between the two groups is very low, which is in agreement with the values of density found for the sample. Thus, safety assessment of new and existing timber structures can be made with similar mechanical data.

With respect to the usage of NDT for the prediction of the ultimate strength, the dispersion found for the density, Resistograph and Pilodyn do not recommended the usage of the related parameters for quantitative mechanical assessment. On the contrary, ultrasonic testing provides good correlations. Novel linear regressions have been proposed in this study.

The different failure mechanisms observed in the experiments are well captured by the model, which is the most important validation of any simulation. It is striking that such excellent agreement is obtained also in the load-displacement diagrams.

A preliminary analysis considering an infinite stiffness of the interface, assuming a fully rigid connection, indicates that such an assumption provides too stiff results. Another conclusion is that the normal stiffness of the interface elements has considerable influence in the yield strength of timber joints. The numerical

results, in terms of force-displacement diagrams, with the adjusted stiffness for the interface elements, provide very good agreement with the experimental results both in the linear and nonlinear parts. The influence of the experimental horizontal restraint, simulated by a linear spring, is only marginal.

It has been shown that the parameters that affect most the ultimate load are the compressive strength of wood perpendicular to the joint and the normal stiffness of the interface elements representing the contact between rafter and brace. The tangential stiffness of interfaces and the Young's moduli of wood have only very limited influence in the response. The compressive strength of wood parallel to the grain has almost no influence in the response.

REFERENCES

Ross, R., DeGroot, R., Nelson, W., Lebow, P., 1997 – "The relationship between stress wave transmission characteristics and the compressive strength of biologically degraded wood". Forest Products Journal, Vol. 47(5), pp. 89–93.

CEN; 1991 – "EN 26891 – Timber structures. Joints Made With Mechanical Fasteners General principles for the determination of strength and deformation characteristics". Office for Official Publications of the European Communities. Brussels, Belgium.

Feio, A., Machado, J., Lourenço, P., 2005 – Compressive behaviour and NDT correlations for chestnut wood (Castanea sativa Mill).

Lourenço, P., 1996 – Computational strategies for masonry structures. PhD thesis, Delft University of Technology.